Int. J. Heat Mass Transfer. Vol. 26, No. 9, pp. 1289–1297, 1983
Printed in Great Britain

0017-9310/83 $3.00 + 0.00

MASS TRANSFER ACROSS A SHEARED, WAVY AIR–WATER INTERFACE

YORAM COHEN
Department of Chemical Engineering, and National Center for Intermedia Transport Research, University of California, Los Angeles, CA 90024, U.S.A.

(*Received* 23 *July* 1982 *and in final form* 3 *January* 1983)

Abstract—The influence of surface motion on liquid phase controlled mass transfer is reviewed. The influence of surface waves and water drift current on air–water exchange was explored theoretically and experimentally, in a laboratory wind-wave facility. The results were analyzed by a surface renewal model. It was found that capillary waves contributed significantly to the enhancement of mass transfer rates at low water friction velocities (for $U_w^* \lesssim 1.5\ \text{cm s}^{-1}$). At higher friction velocities, the rather spectacular increase in mass transfer was associated primarily with the turbulent water drift current. A convenient correlation is proposed for the liquid phase mass transfer coefficient with the water side friction velocity as the only hydrodynamic parameter. This correlation describes both laboratory and *in situ* data satisfactorily.

NOMENCLATURE

A_0	constant in equation (24)
A	wave amplitude
a', a'', a_0	scaling constants in equations (14), (18) and (20), respectively
b'	scaling constant in equation (14)
C_D	wind stress coefficient defined by equation (26)
D	molecular mass diffusivity
E_{ij}	rate of strain tensor
$(e_{ij})_S$	mean rate of strain due to the wind stress
$(e_{ij})_T$	mean rate of strain induced by waves
k	von Kármán constant, equation (22)
K_L	liquid side mass transfer coefficient
l	Kolomogorov eddy length scale
s	surface renewal rate
Sc	Schmidt number, ν/D
U	velocity
U_{10}	wind velocity measured at a height of 10 cm or 10 m in the laboratory and *in situ*, respectively
U_a^*	friction velocity (air side)
U_w^*	friction velocity (water side)
v	root mean square of the velocity fluctuations
y	distance below the water surface
Z	distance above the water surface
Z_0	roughness height, air side

Greek symbols

ε	rate of turbulent energy dissipation
$\varepsilon_d, \varepsilon_s, \varepsilon_w$	contributions of drift current, mechanical mixing and surface waves to the rate of turbulent energy dissipation, respectively
κ	radian wave number, 2π/wavelength
ν	kinematic viscosity
ν_a, ν_w	kinematic viscosities of air and water
ρ_a, ρ_w	densities of air and water
σ	radian frequency, 2π/wave period
τ_w	interfacial shear stress
ω_{ij}	vorticity tensor
$\overline{\omega^2}$	mean square vorticity

1. INTRODUCTION

STUDIES which consider the effect of surface motion and the hydrodynamic interaction of flowing gas and liquid phases on liquid phase controlled mass transfer can be divided into four categories:

(1) One or both phases moving with a hydrodynamically smooth interface.
(2) Mechanically generated instabilities on a stationary or moving liquid phase.
(3) Mechanically generated waves.
(4) Waves and drift current in the liquid phase induced by a co-current turbulent gas flow.

The last category is of particular interest in industrial two phase flow operations as well as in natural water bodies. For example, gas flow induced waves and currents occur in annular and stratified two phase flow in pipes [1], vertical and horizontal film evaporators and gas–liquid separators [1]. Moreover, gas flow induced waves may occur locally in two phase flow situations even though the wavy nature of the flow may not be apparent macroscopically. Finally, surface waves (known as wind waves) are a usual occurrence in environmental water bodies.

In the past, a limited number of studies on the influence of flow induced surface waves on mass transfer have dealt with either thin liquid films, or deep liquid bodies. In the case of thin films, a strong interaction between the wall bounded and free surface shear flows is expected since the induced current extends to several centimeters below the interface. Consequently, the uncoupled effect of the surface region is not understood [2]. Studies on mass transfer in deep water bodies are ideal for elucidating the role of surface waves; hence environmental transport rates.

Theoretical predictions of the liquid phase mass transfer coefficient, K_L, at natural air–water interfaces have been based upon either momentum–mass transport analogies [2–5] or roll cell models [6]. Predictions based on the above methods do not quantitatively portray the variation of K_L with wind speed for laboratory and field data. In addition, the correlations which have been proposed [3–10] have not been rigorously tested over a wide range of conditions. Consequently, there is a need for improving our understanding of mass transfer across wavy sheared gas–liquid interfaces.

In this work, results from a laboratory air–water wind-wave tank are used to investigate the dependence of the liquid side mass transfer coefficient on wind waves and induced water currents.

1.1. *Wind waves: effect of mass transfer*

The term 'wind-waves' refers to the wave field generated by the flow of an air stream over a water body. Here the attention is restricted to mass transfer in water bodies that are at least 1 ft deep, as opposed to the thin films mentioned previously.

The effect of wind–water interaction on gas absorption in laboratory wind-wave tanks and *in situ* (lakes, oceans) has been studied by several researchers [5, 7–19]. These authors generally reported the experimental mass transfer coefficients as a function of the wind velocity U_{10} measured at a height of 10 m (for *in situ* studies) or 10 cm (laboratory wind-wave tanks) above the water surface. As an illustration the results from several studies are shown in Fig. 1. (Some data points have been omitted for clarity.) The noticeable feature is the substantial increase in the liquid side mass transfer coefficient, K_L, by as much as an order of magnitude, in the wind velocity range from 3 to about 10 m s^{-1}. In this region there is an appreciable wave growth and the air flow is aerodynamically rough [20–26]. The corresponding increase in the surface area is believed to be much less than 50% [4, 5, 7, 24]. Hence, the surface area increase alone cannot account for the dramatic mass transfer enhancement.

A consistent feature of the existing studies to date on the role of wind–water interaction on gas exchange is the significant scatter in the reported data (see Fig. 1, also refs. [27, 18]). Evidently the wind velocity is not a sufficient correlating parameter as has been pointed out in several recent studies [3–7].

Above a wind velocity of about 10 m s^{-1}, wave breaking may occur [20–22, 24–26]. A further increase in K_L is expected due to the enhanced mixing of the surface region [5, 7, 25, 26], bubble entrainment, the presence of spray and the disintegration of wave crests [5, 7]. Experimental mass transfer data is lacking in the breaking wave regime. Therefore, the effect of breaking waves cannot be quantitatively assessed at the present time.

In this study the role of breaking waves in gas absorption is not considered since significant wave breaking was not encountered at the range of wind speeds considered here. The present study deals only with the effect of non-breaking waves and wind-induced water currents.

A discussion of the complex wind–water interaction and the resulting effect on the aqueous phase hydrodynamics is beyond the scope of this paper. Detailed discussion of this topic may be found elsewhere [20–26].

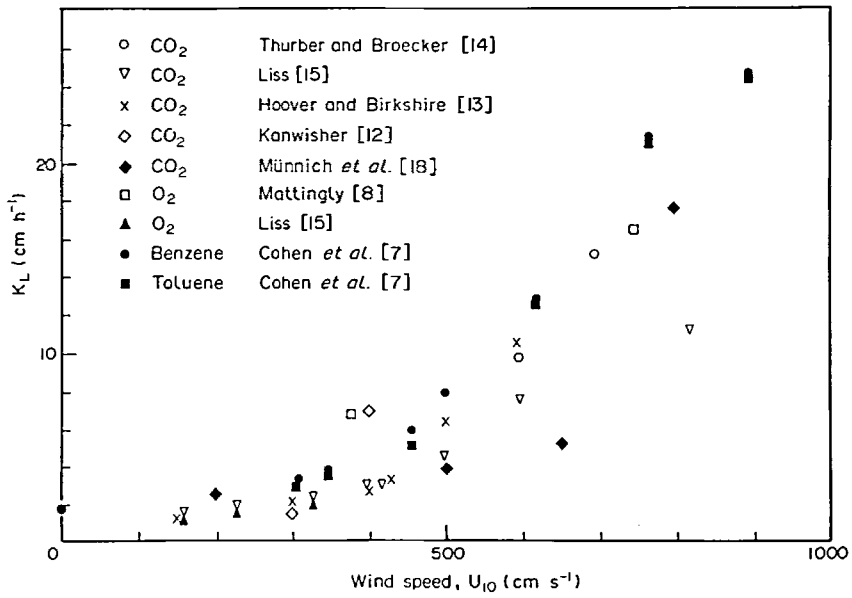

FIG. 1. Liquid phase mass transfer coefficient, K_L vs wind velocity U_{10} (measured 10 cm above the water surface).

2. THE PROPOSED SURFACE RENEWAL CORRELATION

The separate effects of waves and interfacial shear on K_L were considered by Banerjee *et al.* [28, 29] for thin liquid films by using a simple surface renewal model [30]. In this work, the combined effect of wind generated waves and water drift current on K_L is explored by using a similar surface renewal model.

According to the surface renewal model, the liquid side mass transfer coefficient is given by

$$K_L = (Ds)^{1/2} \tag{1}$$

where s is the rate of surface renewal. The renewal rate, s, may be related to the eddy frequency by [31]

$$s \propto v/l, \tag{2}$$

in which v may be taken to be the RMS velocity fluctuation perpendicular to the interface in the interfacial region. The parameter l is the mixing length which characterizes the mass transfer process.

If it is assumed that the rate of mass transfer is controlled by diffusion into the smallest eddies, then l and v may be approximated by the Kolmogorov microscales [32],

$$v = (v\varepsilon)^{1/4}, \tag{3}$$

$$l = (v^3/\varepsilon)^{1/4}, \tag{4}$$

in which ε is the rate of energy dissipation per unit mass at the Kolmogorov microscale. By combining equations (1)–(4), the following expression is obtained for K_L:

$$K_L = aSc^{-1/2}(\varepsilon v)^{1/4} \tag{5}$$

where a is a scaling constant which according to the small eddy roll cell model [33] is about 0.4 for a free surface. In order to utilize equation (5), the rate of energy dissipation, ε, may be calculated from the relation [32]

$$\varepsilon = -v(\overline{\omega^2}) \tag{6}$$

where $\overline{\omega^2}$ is the mean square vorticity just outside the viscous sublayer at the interface. Equation (6) is consistent with the assumption that the isotropic Kolmogorov scale eddies are responsible for much of the viscous dissipation. The mean square vorticity, $\overline{\omega^2}$ can be estimated from the time averaged vorticity equation [32]. In the absence of secondary flows and acceleration effects, the generation of vorticity is balanced by the viscous dissipation,

$$\overline{\omega_i\omega_j E_{ij}} = -\overline{2v\omega_i\nabla^2\omega_i}. \tag{7}$$

If local isotropy is assumed then it can be shown that [24, 34]

$$\overline{2v\omega_i\nabla^2\omega_i} \sim (\overline{\omega^2})^{3/2}. \tag{8}$$

Hence

$$\overline{\omega_i\omega_j E_{ij}} \sim (\overline{\omega^2})^{3/2}. \tag{9}$$

It can be shown [24, 21, 34] that the generation of vorticity is principally due to the following contributions to the rate of strain, E_{ij}: (i) $(e_{ij})_T$ the mean rate of strain induced by the wave, and (ii) $(e_{ij})_S$, the mean rate of strain due to the wind stress on the liquid surface. The rate of strain tensor may be approximated by a linear combination of the above two contributions

$$E_{ij} = (e_{ij})_S + (e_{ij})_T. \tag{10}$$

Hence equation (7) can be expressed as

$$[\overline{\omega_i\omega_j(e_{ij})_S} + \overline{\omega_i\omega_j(e_{ij})_T}] \sim (\overline{\omega^2})^{3/2}. \tag{11}$$

The first term on the LHS of equation (11) can be estimated by

$$\overline{\omega_i\omega_j(e_{ij})_S} \sim \overline{\omega^2 \frac{\partial U}{\partial y}}, \tag{12}$$

in which U is the local velocity of the drift current and y is the vertical distance below the interface. The second term on the LHS of equation (11) can be estimated based on the analysis of Phillips [34] which considered the wave to be a progressive sinusoid [24, 26, 34]. According to this model, to within an order of magnitude the second term in equation (11) can be approximated by

$$\overline{\omega_i\omega_j(e_{ij})_T} \sim \overline{\omega^2}(A^2\kappa^2\sigma)\,e^{-\kappa y}, \tag{13}$$

in which A is the wave amplitude, and κ and σ are the radian wave number and frequency, respectively. Equations (10)–(13) can be combined to yield the following expression for $\overline{\omega^2}$:

$$\overline{\omega^2} = a'\left(\overline{\frac{\partial U}{\partial y}}\right)^2 + b'A^4\kappa^4\sigma^2\,e^{-2\kappa y}, \tag{14}$$

in which a' and b' are scaling constants. The local rate of energy dissipation can be expressed via equations (14) and (6) as

$$\varepsilon = -v\left[a'\left(\overline{\frac{\partial U}{\partial y}}\right)^2 + b'A^4\kappa^4\sigma^2\,e^{-2\kappa y}\right]. \tag{15}$$

For the purpose of calculating the mass transfer coefficient, the value of the rate of energy dissipation at the surface region is required. Near the surface $e^{-\kappa y} \to 1$ [24, 35]. Hence, equation (15) simplifies to yield

$$\varepsilon = -v\left[a'\left(\overline{\frac{\partial U}{\partial y}}\right)^2 + b'A^4\kappa^4\sigma^2\right]. \tag{16}$$

The velocity gradient at the surface can be written as

$$\frac{\partial U}{\partial y} = -\frac{\tau_w/\rho}{v} = -\frac{(U_w^*)^2}{v}, \tag{17}$$

in which τ_w is the wind stress on the water surface and U_w^* is the water side friction velocity. This suggests that as an approximation the average velocity gradient in the surface region can be scaled with the friction velocity U_w^*. Consequently $\overline{\partial U/\partial y}$ in the surface region

may be written as

$$\overline{\frac{\partial U}{\partial y}} = -a'' \frac{(U_2^*)^2}{\nu} \tag{18}$$

where a'' is a scaling constant.

The resulting expression for K_L is obtained by combining equations (5), (16) and (18),

$$K_L = aSc^{-1/2}[\nu(\varepsilon_d + \varepsilon_w + \varepsilon_s)]^{1/4}, \tag{19}$$

in which ε_d, ε_w and ε_s are the individual contributions to the total rate of energy dissipation near the surface (ε), associated with the drift current, wave field and mechanical mixing, respectively. The parameters ε_d and ε_w are defined by

$$\varepsilon_d = a_0(U_w^*)^4/\nu, \tag{20}$$

$$\varepsilon_w = b'\nu A^4\kappa^4\sigma^2, \tag{21}$$

in which a_0 is a scaling constant equal to $a'(a'')^2$. Equations (19)–(21) constitute the proposed correlation for K_L with the scaling parameters a, a_0 and b' to be determined empirically.

3. EXPERIMENTAL

The study was conducted in a wind-wave tank, which has been described previously [7]. The water tank was 240 cm long, 60 cm deep and 60 cm wide. A wind tunnel, 5.65 m in length and 60 × 60 cm cross-section, was mounted over the water tank, such that the air flow joined the water surface tangentially. The air flow was produced by an Aerovent (LS-248) orifice ring fan mounted at the downwind end of the tunnel. Screens and grids of thin walled tubes were placed at the downwind and upwind sections of the tunnel respectively, in order to eliminate the swirl motion produced by the fan, and ensure a uniform velocity distribution. A metal screen was placed at the downwind end of the tank to minimize wave reflection.

The water level in the tank was maintained by a constant water level device [36] which enabled the measurement of water evaporation. Provisions were made for stirring the water phase with two Lightnin (model 806) stirrers, positioned symmetrically, one at each end of the tank with the impellers at a depth of 40 cm.

Local wind velocity profiles along the wind-wave tank were measured using a pitot-static tube of Prandtl design which was mounted on a motor driven traversing mechanism. The wave period and height records were obtained using a resistance probe [7, 24] and recorded using a Beckman (Offner RS) oscillograph. The wavelength records were determined photographically and analyzed via a semi-automatic 'Datalogger' system.

The study of liquid phase controlled mass transfer in the present facility has been previously reported [7]. The unsteady state volatilization of either benzene or toluene (previously dissolved in the water tank) was followed by monitoring the aqueous hydrocarbon concentration. Experimental runs were carried out for wind speeds ranging from 0 to 11.6 m s^{-1} at stirring speeds of 0 and 540 rpm. Details of the experimental technique and analysis can be found elsewhere [7, 36].

3.1. *Results: hydrodynamic parameters*

3.1.1. *Velocity profiles.* The wind velocity profiles followed the turbulent logarithmic velocity profile [7],

$$U = \frac{U_a^*}{k} \ln \frac{Z}{Z_0} \tag{22}$$

where U_a^* and Z_0 are the friction velocity and effective roughness height (air side) respectively, Z is the vertical distance above the water surface and k is the von Kármán constant, taken to be 0.4 [20]. The values of U_a^* for various wind speeds for this facility [7] were used to determine U_w^*, the water side friction velocity, assuming stress continuity at the interface [37, 38],

$$U_w^* = \left(\frac{\rho_a}{\rho_w}\right)^{1/2} U_a^*, \tag{23}$$

in which ρ_a and ρ_w are the air and water densities respectively.

3.1.2. *Wave properties.* The wave properties, wave height, wave period and amplitude were measured at different stations along the wave tank. These results were then used to determine the average wave properties for the length of the tank. The averaging procedure was done only for the dominant waves, these being the waves having amplitudes at least 10% of the largest waves encountered. The wave properties are given in Fig. 2 as a function of wind speed (U_{10}). Wave measurements were not carried out for wind speeds higher than 9.02 m s^{-1} owing to the limitations of the resistance wave probe. It is emphasized that because of the limited length of the wave tank, fully developed gravity waves were not encountered [20–26]. The wave properties reported in the present study are in reasonable agreement with the studies of Hidy and Plate [22] and Schwartz and Marchello [23] for the equivalent fetch.

4. DISCUSSION

It was pointed out by Cohen *et al.* [7] that the effect of mechanical stirring is to introduce a fairly constant addition to the mass transfer coefficient as a function of rpm. If the small eddy model [equation (5)] is applied at zero wind speed, the rate of energy dissipation ε_s due to stirring is 1.88×10^{-4} cm^2 s^{-3}. This contribution to the total rate of energy dissipation was less than 15% for wind velocities above approximately 300 cm s^{-1}.

With the above value of ε_s, the dependence of the group $K_L Sc^{1/2}$ on the rate of energy dissipation due to stirring and the wave field was first investigated. The variation of $K_L Sc^{1/2}$ with the group $[\nu(\varepsilon_w + \varepsilon_s)]^{1/4}$ in which b' [equation (21)] was taken to be unity, is illustrated in Fig. 3. Below a wind velocity of about

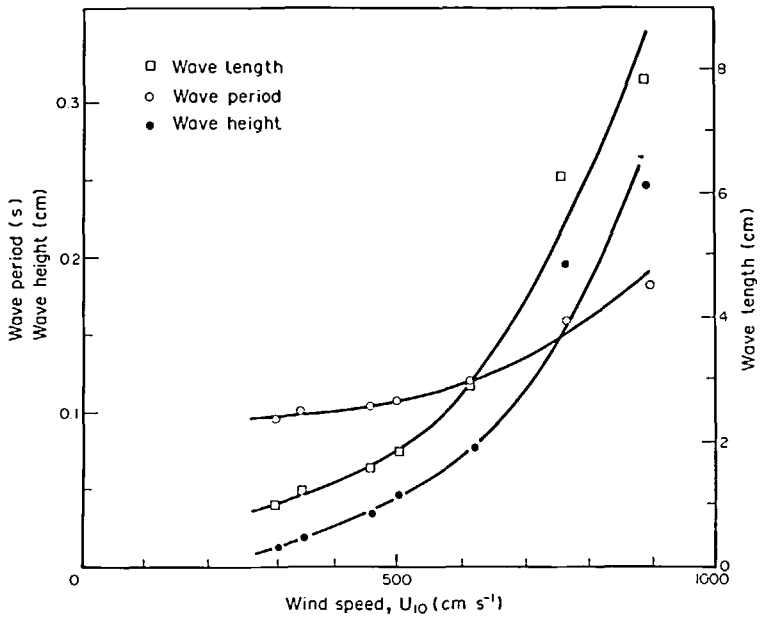

FIG. 2. Variation of wave properties with wind speed [36].

400 cm s^{-1}, a linear relationship holds with a slope of $\sim$0.4 consistent with the value predicted by the small eddy model [see equation (5)].

It must be emphasized that the mass transfer coefficient is not very sensitive to small changes in the rate of energy dissipation due to the 1/4 power dependence on ε [equation (19)]. For example, a 50% error in estimating ε_w at a wind speed of 300 cm s^{-1} results in only a 10% error in predicting the mass transfer coefficient when a value of 0.4 is used for the constant a in equation (19). Hence it appears that a value of unity for b' [equation (21)], and 0.4 for a [equation (19)] are reasonable for the purpose of correlating the data at low wind velocities.

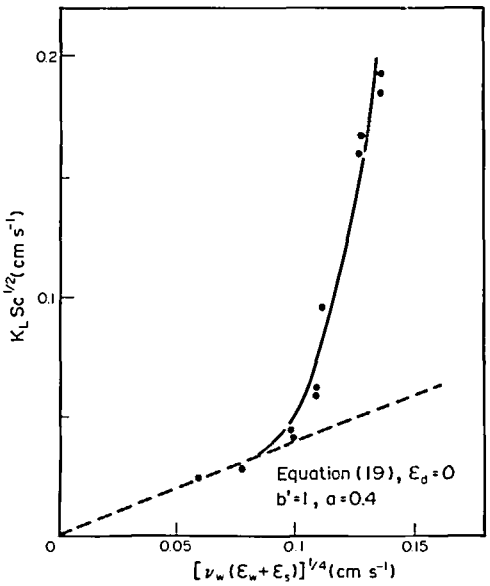

FIG. 3. The dependence of K_L on the rate of energy dissipation due to wave field and mechanical stirring.

Above a wind velocity of about 400 cm s^{-1} the mass transfer coefficient increases rapidly (Fig. 3). At the high wind speeds when only the wave field contribution is considered, the small eddy model does not predict K_L. In order to extend the correlation to higher wind velocities, the rate of energy dissipation associated with the drift current has to be included. Since the scaling constant a_0 [equation (20)] is unknown, this task was carried out empirically by fitting equation (19) to the mass transfer data of Cohen *et al.* [7]. This procedure resulted in a value of 3.25×10^{-4} for the parameter a_0. The average error in the fit of the correlation with the above value for a_0 and the values of 1.0 and 0.4 for b' and a respectively, was 5.5%.

The contribution of the wave field to the total rate of energy dissipation can be determined using the empirical value of a_0. This is shown in Fig. 4 where the fractional contribution of ε_w ($\varepsilon_w/[\varepsilon_w+\varepsilon_d]$) is plotted vs the water side friction velocity, U_w^*. The wave field contribution is most important at low wind speeds where the drift current is weak, and is negligible at high wind speeds where the turbulent energy dissipation is associated primarily with the turbulent drift current.

It was found that ε_w varies approximately linearly with U_w^* while ε_d varies as U_w^{*4}. Hence the contribution of ε_d increases more rapidly with U_w^*. Moreover, since $U_w^* \sim U_{10}^{1.5}$, then $\varepsilon_d \sim U_{10}^6$ and $\varepsilon_w \sim U_{10}^{1.5}$. Hence, $\varepsilon_w/\varepsilon_d \sim U_{10}^{-4.5}$. This behavior indicates a rapid decline in the importance of the wave field contribution to ε, and a greater dependence on the induced drift current and thus, a linear dependence of K_L on U_w^* as the wind speed increases. The contribution of ε_w ranges from about 45

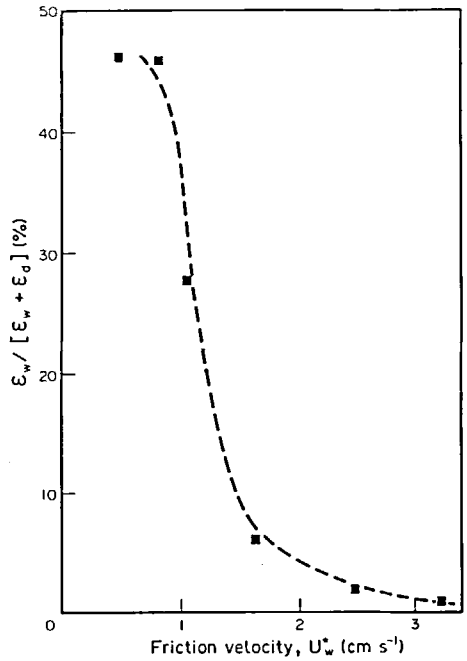

FIG. 4. The contribution (per cent) of the wave field to the total rate of turbulent energy dissipation.

to 1% for the wind velocity range 3–9 m s^{-1}. This is consistent with the conclusion of Wu [20], Stewart and Grant [39], and Snyder *et al.* [40] that about 5–40% of the total momentum flux from the wind is taken up by the wave field.

The role of breaking waves was not considered in this study. Also the current analysis did not allow for any possible interactions between capillary waves and the water drift current. For example, it is known that curvature in the flow direction enhances turbulence [41]. An investigation of the possible significance of breaking waves and wave drift current interactions on gas absorption is currently underway.

4.1. *The correlation*

It was pointed out above that both ε_w and ε_d correlate with the friction velocity U_w^*. It is more convenient to correlate the mass coefficients with U_w^*, especially since wave records are not always available. The resulting correlation is

$$K_L Sc^{1/2} = A_0 + 0.048(U_w^*)^{1.015}\ [\text{cm s}^{-1}] \quad (24)$$

where the parameter A_0 [cm s^{-1}] has the value of 0.0148 for a well-mixed water body. In the absence of mechanical mixing, equation (24) can still be used with a value of 0.0029 for A_0 valid for $U_w^* \leqslant 2$ cm s^{-1}, above which a value of 0.0148 should be used for A_0. The parameter A_0 is related to the degree of mixing other than wind mixing in the particular wind-wave facility. It may be estimated by performing mass transfer measurements at no wind conditions at the desired level of mechanical mixing in the water phase.

Equation (24) fits the experimental data for the benzene and toluene runs of Cohen [36] with an average error of less than 10% up to a U_w^* value of about 4.5 cm s^{-1}. In order to explore the generality of the correlation, its prediction is compared to several laboratory studies in Fig. 8, covering a *Sc* number range of 350–1200. The average friction velocity U_w^* was estimated, for studies which failed to report it, using the correlations recommended by Wu [20, 24], Shemdin [28], and Plate and Hidy [21] as applied to the particular wave-tank facility. The molecular diffusivities were determined based on the data and the recommended Wilke–Chang correlation as reported by Reid *et al.* [43].

The correlation (curves 1 and 2 in Fig. 5) is seen to adequately describe the mass transfer data in

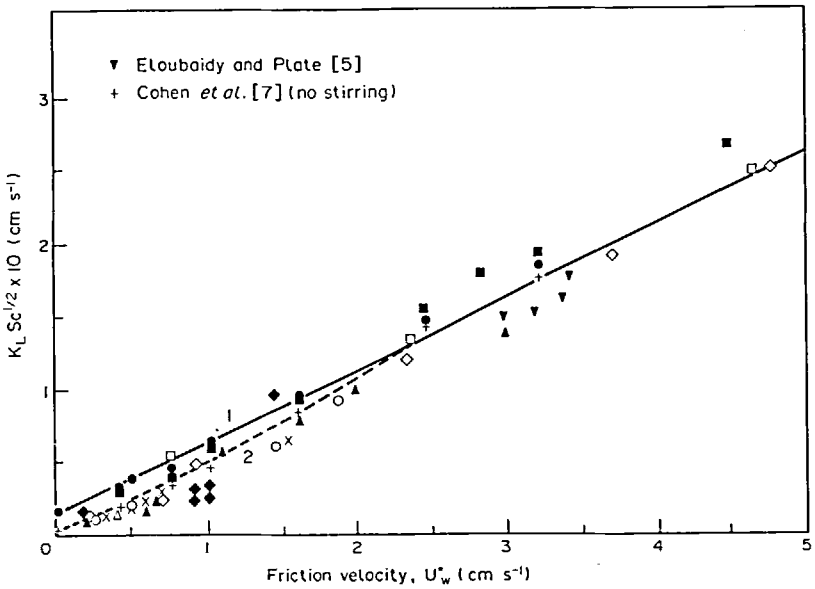

FIG. 5. The proposed mass transfer correlation for K_L. (Legend as in Fig. 1 except as indicated.)

laboratory wind-wave tanks. This is encouraging, especially in view of the incomplete documentation of the experimental conditions in most of the reported studies. At low wind speeds the variation of mechanical mixing (e.g. mechanical mixers, circulating pumps) has a profound effect on the mass transfer coefficient. It appears that curve 1 (stirring at 540 rpm, with $A_0 = 0.0148$) and curve 2 ($A_0 = 0.0029$ no mechanical stirring) represents the approximate upper and lower bounds on the mass transfer coefficients. Data points which fall below curve 2 are believed to correspond to cases of limited drift current and wave growth. It should also be noted that the correlation does not apply when substantial wave breaking occurs.

4.2. *The estimation of K_L in environmental water bodies*

The interest in determining the global transport of nutrients and pollutants requires a quantification of environmental air–water mass transfer. For most gases (e.g. O_2, N_2, CO_2) and many hydrocarbon pollutants [44, 45] the main resistance to transfer is in the liquid phase. For such cases, the correlation as expressed by equation (24) can be used to estimate environmental (*in situ*) K_L values once U_w^* is known as a function of wind speed. This can be accomplished using the commonly reported wind-stress coefficients over the sea surface.

For a fully developed open sea, an accurate multi-formula representation of the wind-stress coefficient was suggested by Wu [42],

$$C_D = 8.5 \times 10^{-4}, \quad U_{10} < 5 \text{ m s}^{-1}, \tag{25a}$$

$$C_D = [0.85 + 0.11(U_{10} - 5)] \times 10^{-3}, \quad 5 \text{ m s}^{-1} < U_{10} < 20 \text{ m s}^{-1}, \tag{25b}$$

$$C_D = 2.5 \times 10^{-3}, \quad U_{10} > 20 \text{ m s}^{-1} \tag{25c}$$

where C_D is the wind-stress coefficient defined as

$$C_D = (U_{10}/U_w^*)^2. \tag{26}$$

Here U_{10} is the wind speed measured at an anemometer height of 10 m. Where the wind-stress coefficient varies with fetch, the methods suggested by Donelan [46] and Wu [42] can be used to estimate the average U_w^* as a function of wind speed over a given water body.

It is well established that U_w^* values in the environment are lower than in the laboratory for the same wind velocity, U_{10} (measured at 10 cm and 10 m above the water surface in the laboratory and *in situ*, respectively [42]). This implies that the present correlation for K_L [equation (24)] should predict lower K_L values in the environment, as is indeed indicated by the laboratory and environment curves in Fig. 6. The comparison of the predicted and available *in situ* K_L values is also shown in Fig. 6. The recent results of Peng *et al.* [19], obtained using the radon deficiency method in the Geosecs Cruises in the Atlantic and Pacific oceans, do not show a definite trend of K_L vs U_{10}. However, a least square fit of the data shows an increase in K_L vs U_{10}, which is substantially less than in laboratory experiments. This is consistent with the prediction of the correlation as is depicted by the environmental curve in Fig. 6.

There appears to be a fair agreement among the predictions of the reported *in situ* results. It is emphasized that the reported *in situ* results are based on measurements over long periods of time during which environmental conditions vary considerably. Thus the available *in situ* K_L values do not provide a definitive test of the proposed correlation. Nonetheless, until more definitive *in situ* data becomes available, the present correlation should be adequate for estimating environmental mass transfer rates.

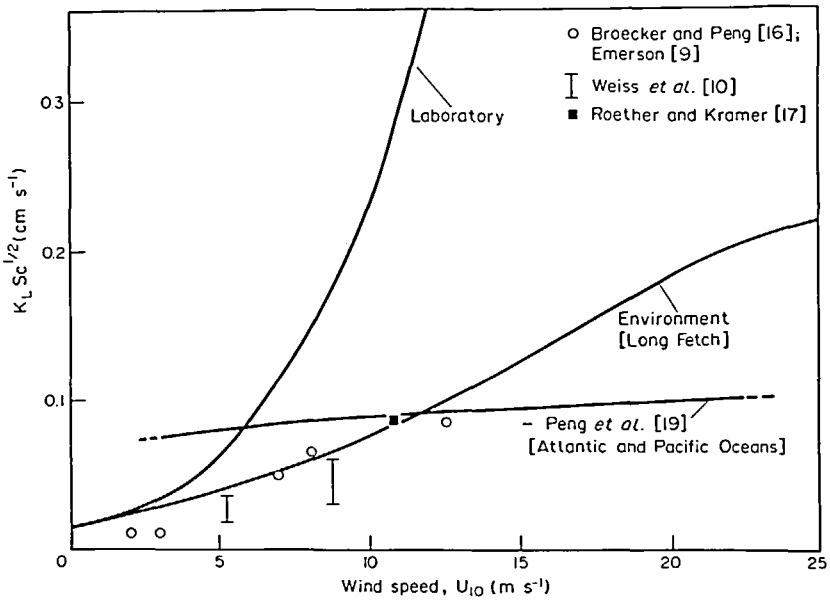

FIG. 6. The prediction of K_L in environmental water bodies.

5. CONCLUSIONS

A surface renewal model provides a coherent description of liquid phase controlled mass transfer across a sheared, wavy air–water interface. The analysis showed that the dramatic mass transfer enhancement at water friction velocities above approximately 1.5 cm s^{-1} is associated primarily with the turbulent wind-induced drift current. At lower friction velocities, the wave field contribution due to wave induced turbulence has an increasing influence. A convenient correlation, with the water side friction velocity as the only hydrodynamic parameter, is proposed. The correlation describes both laboratory and *in situ* K_L data satisfactorily.

Acknowledgements—This work was supported in part by EPA Grant CR-807864-01. The work is based in part on the author's work at the University of Toronto while on a graduate research fellowship from the National Research Council of Canada.

REFERENCES

1. G. F. Hewitt and N. S. Hall-Taylor, *Annular Two-Phase Flow*. Pergamon Press, Oxford (1970).
2. W. H. Henstock and T. J. Hanratty, Gas absorption by a liquid layer flowing on the wall of a pipe, *A.I.Ch.E. Jl* **25**, 122–131 (1979).
3. E. L. Deacon, Gas transfer to and across an air–water interface, *Tellus* **29**, 363–374 (1977).
4. L. Hasse and P. S. Liss, Gas exchange across the air–sea interface, *Tellus* **32**, 470–481 (1980).
5. A. F. Eloubaidy and E. J. Plate, Wind-shear turbulence and reaeration coefficient, *J. Hydraulic Div. ASCE* **98**, 153–170 (1972).
6. W. J. Brkto and R. L. Kabel, Transfer of gases at natural air–water interfaces, *J. Phys. Oceanogr.* **8**, 543–556 (1978).
7. Y. Cohen, W. Coccio and D. Mackay, Laboratory study of liquid-phase controlled volatilization rates in presence of wind waves, *Environ. Sci. Technol.* **12**, 553–558 (1978).
8. G. E. Mattingly, Experimental study of wind effects on reaeration, in *Turbulent Fluxes through the Sea Surface, Wave Dynamics, and Prediction* (edited by A. Favre and K. Hasselman). Plenum Press, New York (1978).
9. S. Emerson, Gas exchange rates in small Canadian shield lakes, *Limnol. Oceanogr.* **20**, 754–761 (1975).
10. W. Weiss, H. Lehn, K. H. Fischer, W. B. Clarke, Z. Top, B. Kromer and W. Roether, Gas exchange and internal mixing of Lake Constance, Verh. Ges. Okobgie, Kiel, September (1977).
11. A. L. Downing and G. A. Truesdale, Some factors affecting the rate of solution of oxygen in water, *J. Appl. Chem.* **5**, 570–581 (1955).
12. J. Kanwisher, On the exchange of gases between the atmosphere and the sea, *Deep-Sea Res.* **10**, 195–208 (1963).
13. T. E. Hoover and P. C. Birkshire, Effects of hydration on carbon dioxide exchange across air–water interface, *J. Geophys. Res.* **74**, 456–464 (1969).
14. D. L. Thurber and W. S. Broecker, The behavior of radiocarbons in surface of waters of the Great Basin, in *Proc. Nobel Symp.* (edited by I. V. Olson), Vol. 12, pp. 379–400. John Wiley, New York (1970).
15. P. S. Liss, Processes of gas exchange across an air–water interface, *Deep-Sea Res.* **20**, 221–238 (1973).
16. W. S. Broecker and T. H. Peng, Gas exchange rates between air and sea, *Tellus* **25**, 21–35 (1974).
17. W. Roether and B. Kramer, Field determination of air–sea gas exchange by continuous measurement of radon-222, *Pure Appl. Geophys.* **116**, 476–485 (1978).
18. K. O. Münnich, W. B. Clarke, K. H. Fischer, D. Flothmann, B. Kromer, W. Roether, U. Siegenthaler, Z. Top and W. Weiss, Gas exchange and evaporation studies in a circular wind tunnel, continuous radon-222 measurements at sea and tritium-helium-3 measurements in a lake, in *Turbulent Fluxes through the Sea Surface, Wave Dynamics, and Prediction* (edited by A. Favre and K. Hasselman). Plenum Press, New York (1978).
19. T. H. Peng, W. S. Broecker, G. G. Mathiu, Y.-H. Li and A. E. Bainbridge, Radon evasion rates in the Atlantic and Pacific oceans as determined during the GEOSECS program, *J. Geophys. Res.* **84**, 2471–2486 (1979).
20. J. Wu, Laboratory studies of wind-wave interaction, *J. Fluid Mech.* **34**, 91–112 (1968).
21. E. J. Plate and G. M. Hidy, Laboratory study of air flowing over a smooth surface onto small water waves, *J. Geophys. Res.* **72**, 4627–4641 (1967).
22. G. M. Hidy and E. J. Plate, Wind action on water standing in a laboratory channel, *J. Fluid Mech.* **26**, 651–687 (1960).
23. R. J. Schwartz and J. M. Marchello, Onset of wind-driven waves, *J. Geophys. Res.* **73**, 5133–5143 (1968).
24. B. Kinsman, *Wind Waves*. Prentice-Hall, Englewood Cliffs, New Jersey (1965).
25. E. J. Plate, Wind-generated water surface waves: the laboratory evidence, in *Turbulent Fluxes through the Sea Surface, Wave Dynamics and Prediction* (edited by A. Favre and K. Hasselman). Plenum Press, New York (1978).
26. O. M. Phillips, *The Dynamics of the Upper Ocean*. Cambridge University Press (1977).
27. R. R. Weiler, Carbon dioxide exchange and productivity in Lake Erie and Lake Ontario, *Verh. Internat. Verein. Kimnol* **19**, 694–704 (1975).
28. S. Banerjee, D. S. Scott and E. Rhodes, Mass transfer to falling wavy liquid films in turbulent flow, *I/EC Fundamentals* **7**, 22–27 (1978).
29. S. Banerjee, D. S. Scott and E. Rhodes, Studies on concurrent gas–liquid flow in helically coiled tubes, *Can. J. Chem. Engng* **48**, 549–551 (1970).
30. P. V. Danckwerts, Significance of liquid-film coefficients in gas absorption, *Ind. Engng Chem.* **43**, 1460–1467 (1951).
31. J. T. Davies, *Turbulence Phenomena*, p. 204. Academic Press, New York (1972).
32. J. O. Hinze, *Turbulence*. McGraw-Hill, New York (1975).
33. J. C. Lamont and D. S. Scott, An eddy cell model of mass transfer into the surface of a turbulent liquid, *A.I.Ch.E. Jl* **16**, 513–519 (1970).
34. O. M. Phillips, A note on the turbulence generated by gravity waves, *J. Geophys. Res.* **9**, 2889–2893 (1961).
35. M. S. Longuet-Higgins, Mass transfer in water waves, *Phil. Trans. R. Soc., London* **A245**, 535–581 (1953).
36. Y. Cohen, Exchange processes across a free air–water interface, M.A.Sc. Thesis, University of Toronto, Toronto, Canada (1976).
37. J. Wu, Wind-induced drift current, *J. Fluid Mech.* **68**, 49–70 (1975).
38. O. H. Shemdin, Wind-generated current and phase speed of wind waves, *J. Phys. Oceanogr.* **2**, 411–419 (1972).
39. R. W. Stewart and H. L. Grant, Determination of the rate of dissipation of turbulent energy near the sea surface in the presence of waves, *J. Geophys. Res.* **7**, 3177–3180 (1962).
40. R. L. Snyder, R. B. Long, F. W. Dobson and J. A. Elliott, The Bight of Abaco pressure experiment, in *Turbulent Fluxes through the Sea Surface, Wave Dynamics and Prediction* (edited by A. Favre and K. Hasselman). Plenum Press, New York (1978).
41. P. Bradshaw, Effects of streamline curvature on turbulent flow, AGARDograph No. 169, Brussels, NATO Advisory Group for Aerospace Research and Development, pp. 45, 80 (1973).
42. J. Wu, Wind-stress coefficients over sea-surface near neutral conditions—a revisit, *J. Phys. Oceanogr.* **10**, 727–740 (1980).

43. R. C. Reid, J. M. Prausnitz and T. K. Sherwood, *The Properties of Gases and Liquids*. McGraw-Hill, New York (1977).
44. D. Mackay and W.-Y. Shiu, The aqueous solubility and air–water exchange characteristics of hydrocarbons under environmental conditions, *Proc. Chem. Phys. Aqueous Gas Solutions* 93 (1975).
45. D. Mackay and Y. Cohen, Prediction of volatilization rates of pollutants in aqueous systems: NBS Symposium on Nonbiological Transport and Transformation of Pollutants on Land and Water, National Bureau of Standards, Gaithersburg, Maryland, May (1976).
46. M. A. Donelan, Are aquatic micrometerologists delivering the goods or is the over-water drag coefficient far from constant?, Manuscript Report Series, No. 43, Symposium on Modeling of Transport Mechanisms in Oceans and Lakes, pp. 325–339, Marine Sciences Directorate, Department of Fisheries and the Environment, Ottawa (1977).

TRANSFERT MASSIQUE A TRAVERS UN INTERFACE AIR–EAU CISAILLE ET ONDULE

Résumé—On considère l'influence du mouvement de la surface sur le transfert massique contrôlé par la phase liquide. L'influence des ondes de surface et des courants de l'eau sur l'échange air–eau est explorée théoriquement et expérimentalement, dans une installation de laboratoire. Les résultats sont analysés par un modèle à renouvellement de surface. On trouve que les onde de capillarité contribuent sensiblement à l'accroissement des flux massiques aux faibles vitesses de frottement (pour $U_w^+ \lesssim 1{,}5\,\mathrm{cm\,s^{-1}}$). Aux plus grandes vitesses, l'accroissement spectaculaire du transfert massique est associé principalement au déplacement turbulent de l'eau. Une formule est proposée pour le coefficient de transfert massique en phase liquide avec la vitesse de frottement coté eau comme unique paramètre hydrodynamique. Cette formule décrit correctement à la fois les données de laboratoire et celles in situ.

DER STOFFÜBERGANG AN EINE WELLIGE LUFT-WASSER-GRENZFLÄCHE BEI SCHERSTRÖMUNG

Zusammenfassung—Der Einfluß der Oberflächenbewegung auf den von der flüssigen Phase bestimmten Stoffübergang wird beschrieben. Die Wirkung von Oberflächenwellen und Wasserströmungen auf den Luft–Wasser-Stoffaustausch wurde theoretisch und experimentell in einer Laboreinrichtung untersucht. Die Ergebnisse wurden anhand eines Oberflächenerneuerungsmodells analysiert. Es wurde festgestellt, daß Kapillarwellen bedeutend zur Steigerung des Stoffübergangs bei geringen Schubspannungsgeschwindigkeiten des Wassers beitrugen ($U_w^* \lesssim 1{,}5$ cm s^{-1}). Bei höheren Schubspannungsgeschwindigkeiten war der erhebliche Anstieg des Stoffübergangs in erster Linie auf die turbulente Driftströmung des Wassers zurückzuführen.

Eine geeignete Korrelation für den Stoffübergangskoeffizienten der flüssigen Phase mit der wasserseitigen Schubspannungsgeschwindigkeit als einzigem hydrodynamischem Parameter wird vorgeschlagen. Diese Korrelation beschreibt sowohl Labor- wie reale Daten befriedigend.

МАССОПЕРЕНОС ЧЕРЕЗ ВОЛНИСТУЮ ГРАНИЦУ РАЗДЕЛА ВОЗДУХ–ВОДА ПРИ СДВИГОВОМ ТЕЧЕНИИ

Аннотация—Рассмотрено влияние движения поверхности на массоперенос в жидкой фазе. Влияние поверхностных волн и сдвигового течения воды на массоперенос между воздухом и водой исследовалось теоретически и экспериментально на лабораторной установке, позволяющей воспроизводить вызываемые ветром волны. Результаты исследований апробированы на модели с обновляемой поверхностью. Найдено, что волны, обусловленные действием капиллярных сил, оказывают существенное влияние на увеличение интенсивности массопереноса при малых скоростях движения воды с трением (при $U_w^* \lesssim 1{,}5$ см с$^{-1}$). При более высоких скоростях довольно заметное усиление переноса массы связано в основном с турбулентным сдвиговым течением воды.

Предложено удобное соотношение для расчета коэффициента массопереноса в жидкой фазе, когда единственным гидродинамическим параметром является скорость перемещения воды. Это соотношение удовлетворительно описывает результаты как лабораторных, так и натурных исследований.